Reassessing the potential of TlCl for laser cooling experiments via four-component correlated electronic structure calculations

Xiang Yuan, André Severo Pereira Gomes

Reassessing the potential of TlCl for laser cooling experiments via four-component correlated electronic structure calculations

Xiang Yuan, André Severo Pereira Gomes

Accepted to J. Chem. Phys. 10.1063/5.0092620

Reassessing the potential of TlCl for laser cooling experiments via four-component correlated electronic structure calculations

Xiang Yuan[1, 2, a)] and André Severo Pereira Gomes[1, b)]
[1)] *Université de Lille, CNRS, UMR 8523 - PhLAM - Physique des Lasers, Atomes et Molécules, F-59000 Lille, France.*
[2)] *Department of Chemistry and Pharmaceutical Science, Faculty of Science, Vrije Universiteit Amsterdam, de Boelelaan 1083, 1081 HV Amsterdam, The Netherlands.*

Following the interest in the experimental realization of laser cooling for thallium fluoride (TlF), determining the potential of thallium chloride (TlCl) as a candidate for laser cooling experiments has recently received attention from a theoretical perspective [X. Yuan et. al. *J. Chem. Phys.*, **149**, 094306, 2018]. From these *ab initio* electronic structure calculations it appeared that the cooling process, which would proceed by transitions between $a^3\Pi_0^+$ and $X^1\Sigma_0^+$ states, had as potential bottleneck the long lifetime (6.04 μs) of the excited state $a^3\Pi_0^+$, that would make it very difficult to experimentally control the slowing zone. In this work, we revisit the electronic structure of TlCl by employing four-component Multireference Configuration Interaction (MRCI) and Polarization Propagator (PP) calculations, and investigate the effect of such approaches on the computed transition dipole moments between $a^3\Pi_0^+$ and $a^3\Pi_1$ excited states of TlCl and TlF (the latter serving as a benchmark between theory and experiment). Whenever possible, MRCI and PP results have been cross-validated by four-component equation of motion coupled-cluster (EOM-CC) calculations. We find from these different correlated approaches that a coherent picture emerges, in which the results of TlF are extremely close to experimental values, whereas for TlCl the four-component calculations now predict a significantly shorter lifetime (between 109 and 175 ns) for the $a^3\Pi_0^+$ than prior estimates. As a consequence, TlCl would exhibit rather different, more favorable cooling dynamics. By numerically calculating the rate equation, we provide evidence that TlCl may have similar cooling capabilities to TlF. Our analysis also indicates the potential advantages of boosting stimulated radiation in optical cycles to improve cooling efficiency.

I. INTRODUCTION

The realization of high-precision measurements on atoms and molecules to verify violation of time-reversal symmetry, for instance the appearance of an electron electric dipole moment (eEDM), has become a valuable tool in the search for new physics outside the Standard Model. This is an alternative method to directly look for new particles in collider experiments, which are currently predicted to require energies on the TeV scale.

To enable such fundamental physics research on atoms and molecules, unprecedented levels of precision in high-precision experiments are essential. Laser cooling technology provides effective means of reducing noise in atomic and molecular spectroscopy, but while widespread for atoms, the cooling of molecules is more challenging. Rosa[1] had outlined the three conditions for molecular candidates in laser cooling : 1) strong one-photon transition, 2) highly diagonal Franck-Condon factors (FCFs) and 3) no intervening electronic state.

Since Shuman, Barry, and DeMille[2] first reported the cooling of the SrF molecule, three diatomic molecules (CaF[3], YO[4], YbF[5]) have been successfully cooled. It is interesting to note that, out of these four successfully cooled systems, three contain atoms for which relativistic effects such as spin-orbit coupling play an important role in the resulting molecular electronic structure. By lifting degeneracies and relaxing selection rules, relativity affects both the energies of electronic states and the associated transition moments. These changes, in turn, provide additional challenges to the design of cooling schemes in comparison to species in the upper rows of the periodic table. Therefore, in this context, simulations based upon relativistic correlated electronic structure calculations, which can achieve rather high accuracy for small, symmetric systems, are particularly interesting as a way to pre-screen candidates for experiments.

Among the species containing heavy elements, thallium halides (TlX) make up an interesting class of systems. TlF is an ideal candidate for measurement of P- and T-violating interactions[6–8] because of its high mass and polarizability. Hunter *et al.*[9] proposed the use of spin-forbidden transition $a^3\Pi_1$-$X^1\Sigma_0^+$ to set up cooling optical cycling for TlF, leading different groups to investigate its spectroscopic properties experimentally[10,11]. More recently, the CeNTREX collaboration[12] has been conducting experiments with ^{205}TlF molecular beams.

The transition used for optical cycling in TlF occurs at 271.7 nm, reflecting the fact that the target $a^3\Pi_1$ excited state is rather high in energy compared to the ground state, potentially making this species less advantageous from an experimental perspective than species in which the target excited states are lower, such as in heavier TlX species. However the calculations of Zou and Liu[13] on TlBr, TlI and TlAt have shown that the potential wells of the target $a^3\Pi$ excited states are not sufficiently aligned with that of ground state to satisfy condition (2). This leaves TlCl as the only remaining candidate along

[a)] Electronic mail: xiang.yuan@univ-lille.fr
[b)] Electronic mail: andre.gomes@univ-lille.fr

this series.

In a recent investigation of the electronic structure of TlCl, Yuan *et al.*[14] arrived at the conclusion that the $a^3\Pi_0^+$-$X^1\Sigma_0^+$ transition would meet the aforementioned conditions for optical cycling. However, their calculated radiative lifetime for the $a^3\Pi_0^+$ state was of about 6 μs, which not only is too long for current experimental conditions, but also at odds with the prior theoretical work by Li *et al.*[15], which found the $a^3\Pi_0^+$ lifetime to be of about 800 ns. Interestingly, in these two investigations the final, spin-orbit coupled electronic states had been obtained from scalar relativistic correlated calculations, whose spin-free states are subsequently coupled via spin-orbit configuration interaction (SOCI) calculations.

Thus, the first objective of this work is to revisit the TlCl system employing more sophisticated relativistic correlated electronic structure methods, in order to resolve the discrepancies in radiative lifetimes described in the literature. With that, our second goal is to address whether or not TlCl can be a system of interest for laser cooling experiments. Given the lack of experimental data on radiative lifetimes for TlCl, we shall also verify the performance of our theoretical approaches with respect to experimental results of the TlF system.

As it is known in the literature[16–20], SOCI calculations can be very sensitive to the number of electronic spin-free states entering the SOCI calculation, and whether a contracted or uncontracted CI is employed. Because of that, we consider it of interest to attack this problem from a different perspective, with spin-orbit coupling (SOC) interactions being accounted for at mean-field level by using four-component based Hamiltonian. That is to be followed by a treatment of electronic correlation in a spinor basis, employing the multireference configuration interaction (MRCI) method as well as benchmark calculations with the relativistic Equation of Motion Coupled-Cluster singles doubles (EOM-CCSD)[21] and the Polarization Propagator (PP)[22] approaches, in order to cross-validate the MRCI calculations for ground, excited and transition properties.

This paper is organized as follows. The details of the *ab initio* calculations are described in section II. The computational results and the corresponding cooling scheme are presented and discussed in section III. Finally a brief summary is presented in section IV.

II. COMPUTATIONAL DETAILS

The *ab initio* calculations on the electronic states of TlF and TlCl have been performed with the DIRAC19[23] and DIRAC22[24] releases, as well as with a publicly available development snapshot (commit hash *e0617189*) of the the DIRAC relativistic electronic structure package[25]. In all calculations we employed the four-component Dirac-Coulomb(DC) Hamiltonian, with the usual approximation of the $(SS|SS)$ integrals by a Coulombic correction[26]. The uncontracted Dyall basis sets aae$n$Z[27] were employed for Tl atom, and the correlation-consistent basis set aug-cc-pVnZ[28,29] were employed for the halogens. In both cases n is the basis sets cardinal number ($n = 2, 3, 4$ for double-, triple-, and quadruple-zeta respectively). As a shorthand notation, in the following we shall refer to the different basis sets as nZ.

The molecular axis is placed along the z-axis with the center of mass at the origin, with the positive direction being from Tl to X. For permanent dipole moments (PDM), we used the following bond lengths (in Å) corresponding to the experimental equilibrium distances: 2.0844 ($X^1\Sigma_0^+$, TlF), 2.049 ($a^3\Pi_0^+$, TlF), 2.0745 ($a^3\Pi_1$, TlF), 2.485 ($X^1\Sigma_0^+$, TlCl), 2.472 ($a^3\Pi_0^+$, TlCl), 2.485 ($a^3\Pi_1$, TlCl). Since, the PDM of a linear molecule is the first derivative of the energy with respect to the electric field along the molecular z-axis, in the complete basis set (CBS) limit, the ground state PDMs are obtained via an expression analogous to that for the total energy[30], that is:

$$\mu_{CBS} = \mu_n - \alpha \exp^{-(n-1)} - \beta \exp^{-(n-1)^2}, \qquad (1)$$

for which results from 2Z, 3Z and 4Z basis sets calculations are needed. We note that for excited states, the CBS results are extrapolated based on 3Z and 4Z results with the formula[20,31]:

$$E_{CBS}(\mathbf{R}) = \frac{4^3 E_4(\mathbf{R}) - 3^3 E_3(\mathbf{R})}{4^3 - 3^3}. \qquad (2)$$

In this study, we focused on the transitions of $a^3\Pi_1$-$X^1\Sigma_0^+$ and $a^3\Pi_0^+$-$X^1\Sigma_0^+$ ($\Omega = 0$ states) of TlF and TlCl. The PDMs and the transition dipole moments (TDMs) were obtained with the MRCI method as implemented in the KRCI module[32,33] (we note the KRCI module employed in our calculations does not support the use of two-component Hamiltonians). In the MRCI calculations, the base configuration space is defined as (8,8) corresponding to the 6s, 6p and 7s orbital of Tl and 2(3)p orbitals of halogen. The detailed Generalized Active Spaces (GAS) used in these KRCI calculation, including the number of configurations–as well as the GAS setups for additional calculations aiming to verify the robustness of transition moment values with respect to active space–are presented in the supplemental material.

We have also carried out calculations of excitation energies, PDMs and TDMs with the four-component CCSD[34,35], EOM-CCSD [36] and PP[37,38] methods. The analytic calculation of excited state expectation values is currently not possible for both methods in their implementations in DIRAC. Due to that, we obtained excited state dipole moments through finite field calculations. In these, the component of the dipole moment operator are individually taken as the perturbations (with strengths of ± 0.0005 a.u) and are included at the Hartree-Fock step, corresponding to an orbital-relaxed picture. We note that for the EOM-CCSD implementation, the transition dipole moments are also not currently available. In

contrast, for PP these are available and will be compared to those obtained with MRCI. For EOM-CCSD and PP, we explored different correlation spaces, in order to verify the effect of truncation: we consider occupied orbitals with energies higher than -10 a.u. or -20 a.u. and virtual orbitals with energies up to and including 20 a.u. or 100 a.u.

The data, figures and scripts associated to this paper all can be obtained as supplemental information in the Zenodo repository[39].

III. RESULT AND DISCUSSION

A. Permanent dipole moment

We present in Table I the PDMs and vertical excitation energies (T_v) for MRCI, EOM-CCSD, and PP, alongside the SOCI calculations from the literature[14,40] and the experimental results[10].

We find that EOM-CCSD results are rather insensitive to the increase of the correlating space (from -10 to 20 a.u., to -20 to 100 a.u.) for both the 2Z and 3Z (changes are less than 100 cm^{-1}), whereas for PP there are more significant changes for the 2Z set (1000 cm^{-1}), but these fall largely in line with the EOM-CCSD results for the 3Z basis sets. With that, by considering the 3Z basis set results in the following discussion, the same semi-quantitiative trends will apply for both correlating spaces, and for convenience (and unless otherwise noted) we shall refer to the smaller orbital space (-10 a.u. to 20 a.u.) results.

For the MRCI PDMs, our results indicate an asymptotic convergence as a function of basis set level for all states under consideration. This translates into a decrease in the magnitude of dipole moments for all states of TlF and TlCl at the CBS level, compared to the results obtained with the smaller basis sets. Furthermore, the magnitudes of the dipole moments of the excited states are smaller than those of the ground states, and the magnitudes of the PDMs for TlF are all smaller than those for TlCl. In all of our results the PDMs possess a negative sign, meaning that a decrease in magnitude correlates to a build-up in electronic density surrounding the Tl atom as the quality of the basis set is enhanced.

The MRCI results are consistent with the coupled-cluster results (due to computational resource limitations, we were unable to perform EOM calculations with 4Z bases, and thus only present results for 2Z and 3Z bases); the differences in PDMs between the two approaches are typically, in absolute value, between 0.3 and 0.5 D for all states considered. It is interesting to note that variations across approaches tend to be lower for 3Z bases than for 2Z bases, with the coupled-cluster findings deviating less than MRCI ones when shifting from 2Z to 3Z; hence, we expect that our 3Z results can serve as a semiquantitative comparison, and give us with confidence that our 4Z and CBS MRCI results are reliable.

For the coupled-cluster ground states, for which we can also calculate PDMs analytically, we observe that the finite-field and analytic derivative results are very close (differences around 0.03-0.04 D), indicating that (a) orbital relaxation is not particularly important for such species and (b) the finite-field results for the various electronic states are reliable. We furthermore reuse the results from the finite-field calculations to evaluate the α_{zz} components of the polarizability, which are listed in Table S3 in the supplementary information and find that the value of TlCl (191 a.u.) is almost twice as large as that of TlF (110 a.u.). These results suggest that, in comparison to TlF, TlCl is more easily polarized by the external electric field, which in turn provides more favorable conditions for experiments testing P-T violation.

Finally, we see that for the ground state, the SOCI results of Yuan *et al.*[14] and our MRCI results compare rather well. For excited states, the situation is different, particularly for the $a^3\Pi_1$ state, as we observe significant differences between methods for both TlF and TlCl.

In comparison to the experiment, the PDM measurements of the $a^3\Pi_1$ state of TlF by Clayburn *et al.*[10], which yielded a value of -2.28(7) D, are in very good agreement with our MRCI 4Z (-2.46 D) or CBS (-2.47 D) results, as well as our EOM-CCSD 3Z results (-2.47 D). From that, and the very similar MRCI and CCSD results for TlCl, we expect that our calculations do provide a good estimate of the experimental value. We believe future high-resolution PDM measurements for more states would be highly desirable as a test, and possible confirmation, of our results.

Concerning the vertical excitation energies (T_v), for TlF we observe significant variations with the basis set size for MRCI, which result in decreasing excitation energies as the basis sets quality is improved (roughly a 2000 cm^{-1} decrease when passing from 2Z to 3Z for both $^3\Pi$ states, and nearly 1000 cm^{-1} when passing from 3Z to 4Z, and another 1000 cm^{-1} when passing from 4Z to CBS). This tendency is qualitatively the same in the EOM-CCSD calculations, although the changes are somewhat smaller (about 300-400 cm^{-1} from 2Z to 3Z).

On the other hand, for MRCI results on TlCl we see significantly smaller fluctuations with changing basis sets (less than 1000 cm^{-1} between 2Z and CBS values), with increasing excitation energies as basis sets are improved. As for TlF, EOM-CCSD trends mirror those of MRCI, and energy changes with respect to basis sets are again less significant than those for MRCI.

In contrast to MRCI and EOM-CCSD, PP results for all excited states demonstrate an increase in excitation energies with improving basis set size, with changes between 2Z and 3Z of around 1000 cm^{-1} for the smaller correlating space, but around 300 cm^{-1} for the larger correlating space. It is interesting to observe that the 3Z PP excitation energy for both molecules are generally lower but not dissimilar to the MRCI CBS values, though this may be due to fortuitous error cancellations.

However, for TlCl, it appears that all three correlated

techniques exhibit much more similar performance, and in particular PP results are much closer to EOM and MRCI ones.

We see that for both species, the T_v EOM-CCSD results are very much in line with the experimental T_e values (given the nature of the excited states, the calculated T_v values should in effect be quite close to the T_e ones), and since MRCI energies tend to closely follow the EOM-CCSD ones, we consider MRCI energies to reliably reflect experimental excitation energies.

The difference between SOCI and the current four-component derived excitation energies for TlF is striking, with SOCI overestimating the four-component results by 2000 to 3000 cm^{-1}, depending on the excited state. Taken together with the (a) strongly underestimated magnitude of the excited state dipole moment with respect to experiment; and (b) the rather good agreement for calculated ground-state dipole moments, it would appear that the SOCI calculations of Liu *et al.*[40] are somewhat unbalanced in their descriptions of the excited states, with respect to the ground-state. Interestingly, for TlCl, the four-component excited state energies, as well as the ground and excited state dipole moments, agree pretty well with the SOCI estimates. This shows that any problems with SOCI calculations are not so much in the description of the different electronic states of TlCl, but rather in the transition properties, to which we will now shift our attention.

B. Transition properties

Our results for TDMs, obtained at bond lengths corresponding to the experimental excited states' equilibrium distances, are found in Table II. Unlike excited state properties, CBS values cannot be estimated for TDMs; hence, we chose to focus on MRCI TDM data obtained with 4Z basis sets.

Before discussing these results, we have carried out a number of MRCI calculations with different GAS definitions (employing 3Z basis sets due to constraints on computational resources). Our aim with these was to investigate whether or not TDM values vary significantly upon including configurations correlating outer core electrons (the 5d orbitals of Tl) and increasing the virtual space to include higher-lying virtuals (i.e. those with energies up to and including 30 a.u.), than those we were able to consider in the 4Z calculations.

From our results, found in the supplementary information (Tables S4 and S5, and Figure S1), we observe first that core correlating configurations tend to increase the TDMs, but not so drastically. This decrease is more significant (around -0.13 D) for calculations employing the larger virtual space than for those employing the smaller virtual space (around -0.07 D). Consequently, outer-core correlation has an impact on the calculated lifetimes: these change from 163 ns to 137 ns for the calculations with smaller virtual space, and from 145 ns to 109 ns for the calculations with the larger virtual space.

At the same time, we observe that core correlating configurations tend to increase excitation energies, making them move away from the experimental value. As was the case for the TDMs, this effect is more pronounced for the calculations with the larger virtual space ($+2333$ cm^{-1}) than with the smaller virtual space ($+862$ cm^{-1}). By inspecting Figure S1, we observe that the presence of core correlating configurations tends to preferentially stabilize the ground state with respect to the excited state.

We note the 3Z results are in agreement with the trend observed for the comparable 4Z calculations. With this, and the effect of core correlating configurations in mind, we consider our valence 4Z calculations can provide, respectively, a lower bound for the TDMs and an upper bound for the lifetimes in TlCl.

As EOM TDMs are not yet accessible, we present TDMs values derived from 4Z PP calculations; based on its similarity to EOM and MRCI results for TlCl, we anticipate that PP calculations provide sufficiently accurate results to serve as a cross-validation of MRCI results, though somewhat less so for TlF. As for the case of transition energies, we have also assessed the effect of the correlation space truncation on the PP TDMs between the ground and $a^3\Pi_1$ state of TlF, and the ground and $a^3\Pi_0^+$ excited state of TlCl. We find that the results do not vary substantially, which we take as a further indication that for these systems the TDMs value are not very sensitive to the truncation of the orbital space.

We find that for different transitions in TlF, the MRCI and PP results are indeed quite close to each other, differing by less than 0.1 D for the transitions from the ground to each of the Ω components of the Π states. We note that for the transition to the $a^3\Pi_0^+$ state, the PP TDM is larger than the MRCI one, whereas the reverse is true for the transition to the $a^3\Pi_1$ state.

As for TlF, for TlCl the difference between MRCI and PP is slightly larger than 0.1 D for the transition from the ground state to the $a^3\Pi_0^+$ state, and the PP value is again larger than the MRCI one. We note here that the PP results are, on the other hand, quite similar to the largest 3Z MRCI calculations including core correlating configuration. This could be a further indication that the actual lifetimes could indeed be somewhat lower than the 175 ns obtained from valence 4Z MRCI calculations, since in the PP calculations the 5d Tl electrons are also correlated.

The good agreement between these two four-component techniques for both molecules, with results differing by no more than 25%, makes us confident in the capability of MRCI to generate sufficiently accurate TDMs for a reliable assessment of lifetimes, discussed below.

Comparing our current results for TlCl to those in the literature, we observe first that for the transition from ground to the $a^3\Pi_1$ state, our results differ slightly more than 0.1 D from those from Yuan *et al.*[14]. Second, we see that the SOCI TDMs of $a^3\Pi_0^+$ are strongly underes-

Table I. Computed permanent dipole moments (in Debye) and vertical excitation energies (T_v, in cm^{-1}) for the different states under consideration for TlF and TlCl.

			2Z		3Z		4Z		CBS		SOCI[14,40]		Exp	
Molecule	State	Method	PDM	T_v	PDM	T_v	PDM	T_v	PDM	T_v	PDM	T_v	PDM	T_e[c]
TlF	$X^1\Sigma_0^+$	MRCI	-4.16	0	-3.88	0	-3.79	0	-3.74	0	-3.67	0		
		CCSD[a]	-4.37	0	-4.32	0								
		CCSD[b]	-4.33	0	-4.29	0								
		CCSD[b,d]		0	-4.30	0								
	$a^3\Pi_0^+$	MRCI	-3.15	36825	-2.81	34695	-2.76	33708	-2.74	32990	-1.46	37025		35164
		EOM[a]	-2.67	34790	-2.69	35082								
		EOM[d]				35148								
		PP		31592		32414								
		PP[e]		32185		32524								
	$a^3\Pi_1$	MRCI	-2.90	40070	-2.47	37921	-2.46	36507	-2.47	35474	-1.26	38535	-2.28	36864
		EOM[a]	-2.45	36475	-2.47	36782								
		EOM[d]				36851								
		PP		32920		33719								
		PP[e]		33513		33820								
TlCl	$X^1\Sigma_0^+$	MRCI	-4.60	0	-4.46	0	-4.42	0	-4.4	0	-4.32	0		
		CCSD[a]	-4.66	0	-4.65	0								
		CCSD[b]	-4.63	0	-4.64	0								
		CCSD[b,d]	-4.66	0	-4.64	0								
	$a^3\Pi_0^+$	MRCI	-2.43	31130	-2.19	31630	-2.13	31813	-2.1	31947	-2.08	31438		31054
		EOM[a]	-1.78	31095	-1.80	31182								
		EOM[d]		31246		31232								
		PP		30801		31338								
		PP[d]		31072		31380								
	$a^3\Pi_1$*	MRCI	-1.83	33366	-1.51	34594	-1.48	34711	-1.47	34797	-1.74	32526		
		EOM[a]	-1.45	32369	-1.29	32426								
		EOM[d]		32500		32467								

[a] Finite-field calculations, equivalent to an orbital-relaxed formulation.
[b] Analytic gradient calculation, employing an orbital-unrelaxed formulation[35].
[c] Experimental adiabatic excitation energy value
[d] Correlation space : -10 a.u. to 100 a.u.
[e] Correlation space : -20 a.u. to 100 a.u.
* $a^3\Pi_1$ state of TlCl is not a bound state

timated, differing from ours by nearly 0.7 D.

The TDMs of $a^3\Pi_0^+$ and $a^3\Pi_1$ of TlCl are slightly larger than the corresponding MRCI and PP ones for TlF, something which is consistent with our understanding that TlCl should have somewhat stronger spin-orbit coupling effects than TlF, whereby further weakening the selection rules making the spin forbidden transition $a^3\Pi$-$X^1\Sigma^+$ in comparison to TlF.

As the differences in computed TDMs are already illuminating, a more direct comparison to experiment is provided by the lifetimes presented in Table II. From the TDMs, we evaluate the Einstein coefficients from[14]

$$A_{v'v''} = 2.142 \times 10^{10} \times TDM^2 \times q_{v'v''} \times \Delta E^3 \qquad (3)$$

(where the energy difference ΔE and the TDMs are given in a.u. and $A_{v'v''}$ in s^{-1}) while the radiative lifetimes are obtained using

$$\tau_{v'} = \frac{1}{\sum_{v''} A_{v'v''}} \qquad (4)$$

The vibrational energy levels and the corresponding Franck-Condon factors ($q_{v'v''}$) are taken from available experiments[9,41]($a^3\Pi_1$ state of TlF) and prior calculations[14,40]($a^3\Pi_0^+$ state of both TlF and TlCl). The detailed Einstein coefficients $A_{v'v''}$ and vibrational branching $R_{v'v''}$ of transitions are listed in the supplementary material.

Given that SOCI PDMs and four-component PDMs for the ground states of TlF and TlCl match quite well, we consider this method (combining ground-state vibrational wavefunctions derived from SOCI potential energy curves and four-component TDMs at the MRCI or PP level) to be reliable.

For TlF, the computed lifetime of the $a^3\Pi_1$ state is 91 and 153 ns for MRCI and PP, respectively and the former is closer to the experimental value 99(9) ns. For TlCl, the 6.04 μs lifetime of the $a^3\Pi_0^+$ state calculated by Yuan *et al.*[14] would correspond to a huge challenge under current cooling experimental condition. However, we see that on the basis of the current four-component cal-

culations without including outer-core correlation, lifetimes for the $a^3\Pi_0^+$ state would correspond to 175 ns (MRCI) and 128 ns (PP), respectively, which are both much shorter than the previous value, and as discussed above with the inclusion of outer-core correlation, the tendency is for lifetimes to further decrease. From these results, we therefore conclude that TlCl should be a much more favorable system for experimental realization of laser cooling than previously thought.

Given the small deviation between theoretical and experimental lifetimes for the MRCI $a^3\Pi_1$ state of TlF, and the systematic agreement between four-component approaches for TDMs, we thus consider the lifetime of $a^3\Pi_0^+$ state of TlCl 175 ns to be a more accurate (upper bound) estimate than the previous estimation by Yuan *et al.*[14], and shall use this new calculated lifetime in the following assessment of a proposed cooling scheme.

Table II. Computed transition dipole moments at R_e and the corresponding lifetimes

TlF	Transition	TDM(D)	lifetime(ns)	Reference
	$a^3\Pi_1$-$X^1\Sigma_0^+$	0.837	91	MRCI
	$a^3\Pi_1$-$X^1\Sigma_0^+$	0.673	153	PP[a]
	$a^3\Pi_1$-$X^1\Sigma_0^+$	0.634	172	PP[b]
	$a^3\Pi_1$-$X^1\Sigma_0^+$		99(9)	Exp[9]
	$a^3\Pi_1$-$a^3\Pi_0^+$	0.114		MRCI
	$a^3\Pi_1$-$a^3\Pi_0^-$	0.072		MRCI
	$a^3\Pi_{0+}$-$X^1\Sigma_0^+$	0.518	278	MRCI
	$a^3\Pi_{0+}$-$X^1\Sigma_0^+$	0.651	176	PP[a]
TlCl				
	$a^3\Pi_{0+}$-$X^1\Sigma_0^+$	0.767	175	MRCI
	$a^3\Pi_{0+}$-$X^1\Sigma_0^+$	0.896	128	PP[a]
	$a^3\Pi_{0+}$-$X^1\Sigma_0^+$	0.928	119	PP[b]
	$a^3\Pi_{0+}$-$X^1\Sigma_0^+$	0.130	6040	Ref[14]
	$a^3\Pi_{0+}$-$X^1\Sigma_0^+$		808	Ref[15]
	$a^3\Pi_1$-$X^1\Sigma_0^+$	0.946		MRCI
	$a^3\Pi_1$-$X^1\Sigma_0^+$	0.800		Ref[14]

[a] Correlation space : -10 a.u. to 20 a.u.
[b] Correlation space : -20 a.u. to 100 a.u.

C. Simulation of laser cooling

As the cooling efficiency and the corresponding length of the slowing region are dependent on the lifetimes, compared to the results of Yuan *et al.*[14] the new lifetime value for the $a^3\Pi_0^+$ state of TlCl will translate into a different cooling dynamics and, as a result, will alleviate the technological difficulties associated with setting up experiment. In spite of the changes in TDMs, the optical cycling scheme for TlF and TlCl, shown in Fig 1, will still closely follow the one originally proposed by Yuan *et al.*[14], which for the sake of completeness is outlined below.

The main pump laser is set at the $a^3\Pi$(v'=0)-$X^1\Sigma_0^+$(v"=0) transition, with a wavelength $\lambda_{0'0''}$: 272 nm (TlF) and 319 nm (TlCl). Four additional lasers are used to repump the population of vibrationally excited states. For clarity, we refer to these lasers as follows: $\lambda_{0'0''}$ is the first laser, $\lambda_{1'1''}$ is the second laser, $\lambda_{0'2''}$ is the third laser, $\lambda_{1'3''}$ is the fourth laser, and $\lambda_{2'4''}$ is the fifth laser. All the wavelength of the lasers are listed in Table III:

Table III. The wavelength (nm) of lasers used in cooling process represented by figure 1.

laser	TlF	TlCl
1_{st}: $\lambda_{0'0''}$	272	319
2_{rd}: $\lambda_{1'1''}$	273	320
3_{ed}: $\lambda_{0'2''}$	279	325
4_{th}: $\lambda_{1'3''}$	280	326
5_{th}: $\lambda_{2'4''}$	281	327

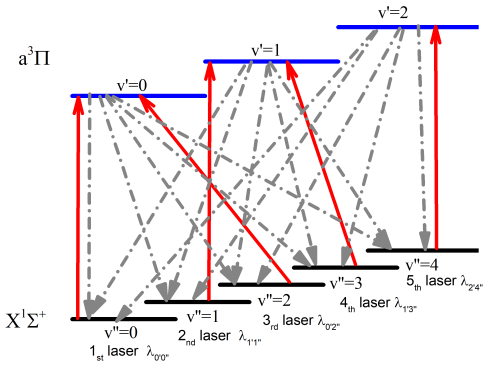

Figure 1. The proposed cooling scheme for TlF and TlCl. The excited states are $a^3\Pi_1$ and $a^3\Pi_0^+$ for TlF and TlCl, respectively. The dashed gray lines are spontaneous decays and the solid red lines are laser-driven transitions.

To discuss the cooling process in more detail, we solve a rate equation to count the number of photons scattered during the cooling process[42]:

$$\frac{\mathrm{d}\mathbf{P}}{\mathrm{d}t} = \mathbf{MP} \tag{5}$$

where $\mathbf{P}$ is a vector holding N vibrational levels in ascending order of energy and M is a N×N matrix containing various Einstein coefficients.

Before simulating the population dynamics, it is necessary to determine the effect of the vibrational decay process on the $X^1\Sigma_0^+$ ground state. Here, we compute the ratio $\frac{A_{0'0''}}{A_{1''0''}}$ of the Einstein coefficient between electronic ($A_{0'0''}$(v'=0) → (v"=0)) and vibrational ($A_{1''0''}$ (v"=1) → (v"=0)) relaxation. The vibrational transition dipole moment (vTDM) matrix elements over vibrational wave functions of $X^1\Sigma_0^+$ state had been computed with the Molcas[31] `vibrot` module.

$$vTDM_{1''0''} = \int \phi_{(v''=1)} R \phi_{(v''=0)} dR \tag{6}$$

The ratio for TlF and TlCl are 1.8×10^7 and 3.0×10^7 respectively. These are similar to the value of 2.5×10^7 for SrF[42]. Such a large ratio indicates that the vibrational relaxation is very weak, thus we chose to exclude it in the subsequent simulation model.

Explicitly, the rate equation has the form:

$$\begin{aligned}\frac{\mathrm{d}P_i}{\mathrm{d}t} = &-\sum_{j=1}^{j=i-1} A_{ij}P_i - \sum_{j=1}^{j=i-1} B_{ij}\rho(\omega_{ij})P_i \\ &-\sum_{j=i+1}^{j=N} B_{ij}\rho(\omega_{ij})P_i + \sum_{j=i+1}^{j=N} A_{ji}P_j \\ &+\sum_{j=1}^{j=i-1} B_{ji}\rho(\omega_{ji})P_j + \sum_{j=i+1}^{j=N} B_{ji}\rho(\omega_{ji})P_j\end{aligned} \tag{7}$$

Here, A_{mn}, B_{ij}, B_{ji} are spontaneous emission, stimulated emission and absorption coefficients, respectively. $\rho(\omega_{ij})$ is the spectral energy density at frequency ω_{ij}.

After numerically solving equation 7, the average number of scattered photons is evaluated by multiplying the obtained population in the excited state of optical cycle by its total radiation rate $A_{ij} + B_{ij}$. The stimulated coefficients B are proportional to A, with

$$B_{ij} = B_{ji} = \frac{\pi^2 c^3}{h\omega_{ij}^3} A_{ij} \tag{8}$$

where h is the Planck constant and c is the speed of light.

In these simulations, we use three different laser configurations : Case **(a-1)** includes three lasers: $\lambda_{0'0''}$, $\lambda_{1'1''}$, and $\lambda_{0'2''}$; Case **(a-2)** has an additional laser $\lambda_{1'3''}$. Case **(a-3)** includes each of the five lasers. The simulation results are plotted in Figure 2. The population is initially in $X^1\Sigma_0^+$ (v"=0) state.

The two molecules show similar dynamics: TlF reaches the limit faster than TlCl, as the rate of its spontaneous radiation is nearly double that of TlCl, while TlCl scatters more photons than TlF does throughout the cooling process. In this model, TlF absorbs roughly 7300 photons when five lasers are utilized, whereas TlCl absorbs 25,000 photons.

A simple equation

$$N_{tot} = \frac{1}{1 - \sum_{i=0}^{i=4} R_{0'i''}} \tag{9}$$

could be used to qualitatively estimate the total photon absorption/emission cycles[43]. It is straightforwad to see N_{tot} is sensitive to the vibrational branching, particularly on the non-diagonal element of Franck-Condon factors such as (v'=0) → (v"=1,2,3...etc). Such sensitivity is also evident in the large difference between the configurations of five and four lasers.

From the discussion above, we have that a smaller number of scattered photons implies the need of a larger number of cooling lasers. This number is in turn dependent on the magnitude of non-diagonal FCFs. It would

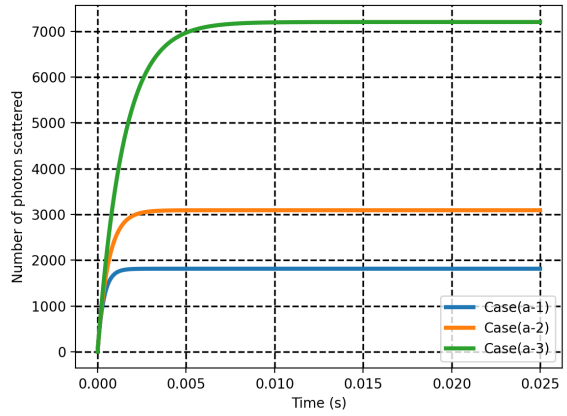

(a) TlF

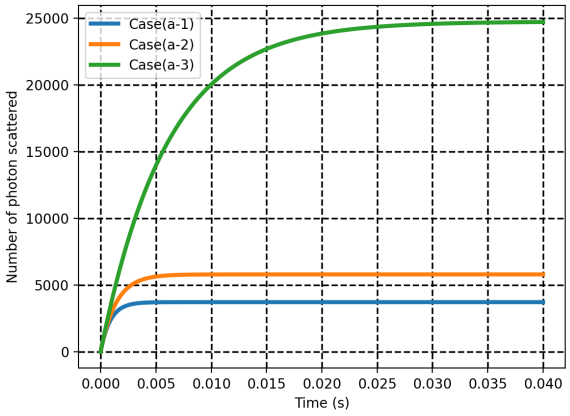

(b) TlCl

Figure 2. The number of scattered photons for TlF and TlCl with different laser configurations. Case **(a-1)** has first three laser: $\lambda_{0'0''}$, $\lambda_{1'1''}$, and $\lambda_{0'2''}$. Case**(a-2)** includes Case **(a-1)**, plus the fourth laser $\lambda_{1'3''}$. Case **(a-3)** includes Case **(a-2)**, plus the fifth laser $\lambda_{2'4''}$.

therefore be of interest, in order to provide the best theoretical estimates for the number of scattered photons, to calculate non-diagonal FCFs at a high level of theory, for instance by including triple and higher excitations to the CI or coupled cluster wavefunctions, considering non-adiabatic corrections, or both.

Due to limitations in both computational resources and availability of computer implementations, it is outside the scope of this work to investigate such aspects. Before attempting to do so, however, it would be useful to have reliable experimental data on vibrational branching measurements in order to determine how much computations must be improved to bridge the gap between theory and experiment for TlCl.

In addition, as reported by Norcia *et al.*[44], introducing the stimulated emission is a potential efficient method

Accepted to J. Chem. Phys. 10.1063/5.0092620

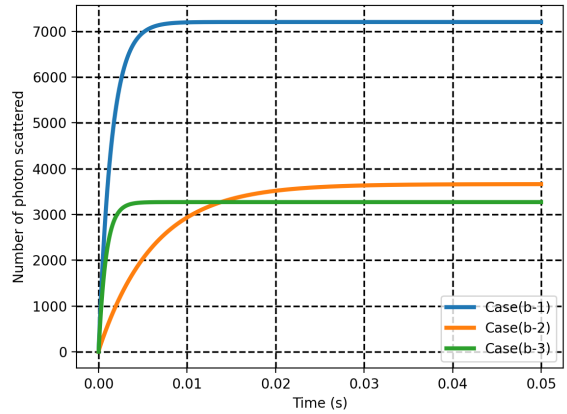

(a) TlF

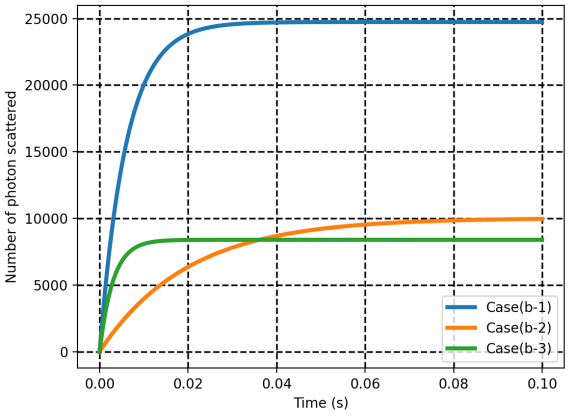

(b) TlCl

Figure 3. The cooling simulation at different levels of stimulated radiation. Case **(b-1)**: spectral energy density $\rho(\omega_{ij})$ is 10^{-12}J/(m^3·s·Hz) ; Case **(b-2)**: $\rho(\omega_{ij})$ is 10^{-13}J/(m^3·s·Hz) ; Case **(b-3)**: $\rho(\omega_{ij})$ is 10^{-12}J/(m^3·s·Hz) but the stimulated radiation coefficients B_{ij} is set as 0.

for laser cooling. Consequently, we also examine the effect of stimulated radiation by varying the spectral energy density $\rho(\omega_{ij})$ of the simulation that employs five lasers. The $\rho(\omega_{ij})$ in Case **(b-1)** and Case **(b-2)** are 10^{-12} J/(m^3·s·Hz) and 10^{-13} J/(m^3·s·Hz) respectively. In Case **(b-3)**, we remove the stimulated radiation terms in the equation and keep the same $\rho(\omega_{ij})$ as for Case **(b-1)**. The results are displayed on Figure 3. The large difference in both photon numbers and scattering rates between Case **(b-1)** and Case **(b-3)** shows that the simulations are significantly affected by stimulated radiation.

By comparing with Case **(b-1)** and Case **(b-2)**, we find that increasing higher spectral energy density results in absorbing more photons. For instance, TlCl could scatter 25000 photons in 0.04 s under $\rho(\omega_{ij}) = 10^{-12}$ J/(m^3·s·Hz) , but only 10000 in 0.08s under $\rho(\omega_{ij}) = 10^{-13}$ J/(m^3·s·Hz). In conclusion, enhancing stimulated radiation is an effective strategy for strengthening the cooling dynamics, including the total number of scattered photons and the scattering rate.

IV. CONCLUSION

Through four-component multi-reference configuration interaction (MRCI), equation of motion coupled-cluster (EOM-CC), and polarization propagator (PP) calculations, we investigated the permanent dipole moments (PDMs) of the ground and low-lying excited states of TlF and TlCl molecules, as well as the transition dipole moments (TDMs) between these electronic states. Our primary objective is to extract, from the TDMs, the excited state lifetimes that will allow us to determine whether or not the TlCl species is a suitable choice for laser cooling experiments.

After cross-validating the four-component MRCI results with the other two methods, we applied it to derive a PDM of -2.47 D and a lifetime of 91 ns for the $a^3\Pi_1$ state of TlF, which are comparable to the experimental results of -2.28(7) D and 99(9) ns, respectively.

For TlCl, we obtained from our four-component MRCI calculations a lifetime of 175 ns for the $a^3\Pi_0^+$ state. This value is much shorter than a recent theoretical estimation of 6.04 μs by Yuan *et al.*[14] from SOCI calculations. Our results point to the strong underestimation by the SOCI method of the TDMs as the main factor behind such a discrepancy, as the SOCI ground and excited state energies and PDMs for TlCl closely match the four-component values.

We have done a comprehensive population simulation with the new lifetime by solving the rate equation, and we find that TlCl exhibits comparable cooling dynamics to TlF. Moreover, our simulations reveal that the vibrational branching of weak transitions driven by non-diagonal elements of Franck-Condon factors may play a significant role in cooling efficiency. We believe that a highly precise experiment measuring the Franck-Condon factors of $a^3\Pi_0^+$-$X^1\Sigma_0^+$ transition of TlCl could provide useful information for pinpointing the deficiencies of current theoretical models.

Finally, we investigate the effect of stimulated radiation on the cooling process. We show that stimulated radiation is significant and that raising the spectral energy density is one approach to enhance the cooling efficiency.

SUPPLEMENTARY MATERIAL

See the supplementary material for further details on the Generalized Active Spaces (GAS) setup and tests of using different MRCI models, the Einstein coefficients and the vibrational branching used in the cooling simulation, and the ZZ component of the polarizability of TlF and TlCl evaluated with finite-field methods.

ACKNOWLEDGMENTS

We thank Valérie Vallet for a critical reading of the manuscript. We acknowledge funding from projects CompRIXS (ANR-19-CE29-0019, DFG JA 2329/6-1), Labex CaPPA (ANR-11-LABX-0005-01) and the I-SITE ULNE project OVERSEE and MESONM International Associated Laboratory (LAI) (ANR-16-IDEX-0004), and support from the French national supercomputing facilities (grants DARI A0090801859, A0110801859).

REFERENCES

[1]M. D. D. Rosa, Eur. Phys. J. D **31**, 395 (2004).
[2]E. S. Shuman, J. F. Barry, and D. DeMille, Nature **467**, 820 (2010).
[3]S. Truppe, H. J. Williams, M. Hambach, L. Caldwell, N. J. Fitch, E. A. Hinds, B. E. Sauer, and M. R. Tarbutt, Nat. Phys **13**, 1173 (2017).
[4]M. T. Hummon, M. Yeo, B. K. Stuhl, A. L. Collopy, Y. Xia, and J. Ye, Phys. Rev. Lett **110**, 143001 (2013).
[5]J. Lim, J. R. Almond, M. A. Trigatzis, J. A. Devlin, N. J. Fitch, B. E. Sauer, M. R. Tarbutt, and E. A. Hinds, Phys. Rev. Lett **120**, 123201 (2018).
[6]E. A. Hinds and P. G. H. Sandars, Phys. Rev. A **21**, 480 (1980).
[7]P. G. H. Sandars, Phys. Rev. Lett. **19**, 1396 (1967).
[8]M. Hubert and T. Fleig, (2022), arXiv:2203.04618.
[9]L. R. Hunter, S. K. Peck, A. S. Greenspon, S. S. Alam, and D. DeMille, Phys. Rev. A **85**, 012511 (2012).
[10]N. B. Clayburn, T. H. Wright, E. B. Norrgard, D. DeMille, and L. R. Hunter, Phys. Rev. A **102**, 052802 (2020).
[11]G. Meijer and B. G. Sartakov, Phys. Rev. A **101**, 042506 (2020).
[12]O. Grasdijk, O. Timgren, J. Kastelic, T. Wright, S. Lamoreaux, D. DeMille, K. Wenz, M. Aitken, T. Zelevinsky, T. Winick, and D. Kawall, Quantum Sci. Technol. **6**, 044007 (2021).
[13]W. Zou and W. Liu, J. Com. Chem **30**, 524–539 (2009).
[14]X. Yuan, S. Yin, Y. Shen, Y. Liu, Y. Lian, H. Xu, and B. Yan, J. Chem. Phys **149**, 094306 (2018).
[15]Y. Li, H. P. Liebermann, G. Hirsch, and R. J. Buenker, J. Mol. Spectrosc **165**, 219 (1994).
[16]V. Vallet, L. Maron, C. Teichteil, and J.-P. Flament, J. Chem. Phys. **113**, 1391 (2000).
[17]A. Weigand, X. Cao, V. Vallet, J.-P. Flament, and M. Dolg, J. Phys. Chem. A **113**, 11509 (2009).
[18]C. Danilo, V. Vallet, J.-P. Flament, and U. Wahlgren, Phys. Chem. Chem. Phys. **12**, 1116 (2010).
[19]A. S. P. Gomes, F. Réal, N. Galland, C. Angeli, R. Cimiraglia, and V. Vallet, Phys. Chem. Chem. Phys. **16**, 9238 (2014).
[20]S. Kervazo, F. Réal, F. Virot, A. Severo Pereira Gomes, and V. Vallet, Inorg. Chem. **58**, 14507 (2019).
[21]R. J. Bartlett, WIREs Comput Mol Sci **2**, 126 (2012).
[22]A. Dreuw and M. Wormit, WIREs Comput Mol Sci **5**, 82 (2015).
[23]*DIRAC, a relativistic ab initio electronic structure program, Release DIRAC19, written by A. S. P. Gomes, T. Saue, L. Visscher, H. J. Aa. Jensen, and R. Bast, with contributions from I. A. Aucar, V. Bakken, K. G. Dyall, S. Dubillard, U. Ekström, E. Eliav, T. Enevoldsen, E. Faßhauer, T. Fleig, O. Fossgaard, L. Halbert, E. D. Hedegård, B. Heimlich–Paris, T. Helgaker, J. Henriksson, M. Iliaš, Ch. R. Jacob, S. Knecht, S. Komorovský, O. Kullie, J. K. Lærdahl, C. V. Larsen, Y. S. Lee, H. S. Nataraj, M. K. Nayak, P. Norman, G. Olejniczak, J. Olsen, J. M. H. Olsen, Y. C. Park, J. K. Pedersen, M. Pernpointner, R. di Remigio, K. Ruud, P. Sałek, B. Schimmelpfennig, B. Senjean, A. Shee, J. Sikkema, A. J. Thorvaldsen, J. Thyssen, J. van Stralen, M. L. Vidal, S. Villaume, O. Visser, T. Winther, and S. Yamamoto see http://www.diracprogram.org* (2019).
[24]*DIRAC, a relativistic ab initio electronic structure program, Release DIRAC22, Written by H. J. Aa. Jensen, R. Bast, A. S. P. Gomes, T. Saue and L. Visscher, with contributions from I. A. Aucar, V. Bakken, C. Chibueze, J. Creutzberg, K. G. Dyall, S. Dubillard, U. Ekström, E. Eliav, T. Enevoldsen, E. Faßhauer, T. Fleig, O. Fossgaard, L. Halbert, E. D. Hedegård, T. Helgaker, B. Helmich–Paris, J. Henriksson, M. van Horn, M. Iliaš, Ch. R. Jacob, S. Knecht, S. Komorovský, O. Kullie, J. K. Lærdahl, C. V. Larsen, Y. S. Lee, N. H. List, H. S. Nataraj, M. K. Nayak, P. Norman, G. Olejniczak, J. Olsen, J. M. H. Olsen, A. Papadopoulos, Y. C. Park, J. K. Pedersen, M. Pernpointner, J. V. Pototschnig, R. di Remigio, M. Repisky, K. Ruud, P. Sałek, B. Schimmelpfennig, B. Senjean, A. Shee, J. Sikkema, A. Sunaga, A. J. Thorvaldsen, J. Thyssen, J. van Stralen, M. L. Vidal, S. Villaume, O. Visser, T. Winther, S. Yamamoto and X. Yuan see http://www.diracprogram.org* (2022).
[25]T. Saue, R. Bast, A. S. P. Gomes, H. J. A. Jensen, L. Visscher, L. A. Aucar, R. R. Di, K. G. Dyall, E. Eliav, E. Fasshauer, *et al.*, J. Chem. Phys **152**, 204104 (2020).
[26]L. Visscher, Theor. Chem. Acc **98**, 68 (1997).
[27]K. G. Dyall, Theor. Chem. Acc **115**, 441 (2006).
[28]R. A. Kendall, T. H. D. Jr, and R. J. Harrison, J. Chem. Phys **96**, 6796 (1992).
[29]D. E. Woon and T. H. D. Jr, J. Chem. Phys **98**, 1358 (1993).
[30]D. Deng, Y. Lian, and W. Zou, Chem. Phys. Lett **688**, 33 (2017).
[31]F. Aquilante, J. Autschbach, A. Baiardi, S. Battaglia, V. A. Borin, L. F. Chibotaru, I. Conti, L. D. Vico, M. Delcey, I. F. Galván, *et al.*, J. Chem. Phys **152**, 214117 (2020).
[32]S. Knecht, H. J. A. Jensen, and T. Fleig, J. Chem. Phys **132**, 014108 (2010).
[33]T. Fleig, J. Olsen, and L. Visscher, J. Chem. Phys **119**, 2963 (2003).
[34]L. Visscher, T. J. Lee, and K. G. Dyall, J. Chem. Phys. **105**, 8769 (1996).
[35]A. Shee, L. Visscher, and T. Saue, J. Chem. Phys. **145**, 184107 (2016).
[36]A. Shee, T. Saue, L. Visscher, and A. Severo Pereira Gomes, J. Chem. Phys. **149**, 174113 (2018).
[37]M. Pernpointner, J. Chem. Phys. **140**, 084108 (2014).
[38]M. Pernpointner, L. Visscher, and A. B. Trofimov, J. Chem. Theory Comput. **14**, 1510 (2018).
[39]X. Yuan and A. S. P. Gomes, "Dataset: Reassessing the potential of tlcl for laser cooling experiments via four-component correlated electronic structure calculations," `https://doi.org/10.5281/zenodo.6376250`.
[40]Y. Liu, X. Yuan, L. Xiao, H. Xu, and B. Yan, J. Quant. Spectrosc. Ra **243**, 106817 (2020).
[41]E. Tiemann, Mol. Phys **65**, 359 (1988).
[42]J. H. V. Nguyen, C. R. Viteri, E. G. Hohenstein, C. D. Sherrill, K. R. Brown, and B. Odom, New. J. Phys **13**, 063023 (2011).
[43]M. Fu, H. Ma, J. Cao, and W. Bian, J. Chem. Phys. **146**, 134309 (2017).
[44]M. A. Norcia, J. R. Cline, J. P. Bartolotta, M. J. Holland, and J. K. Thompson, New. J. Phys **20**, 023021 (2018).

Accepted to J. Chem. Phys. 10.1063/5.0092620

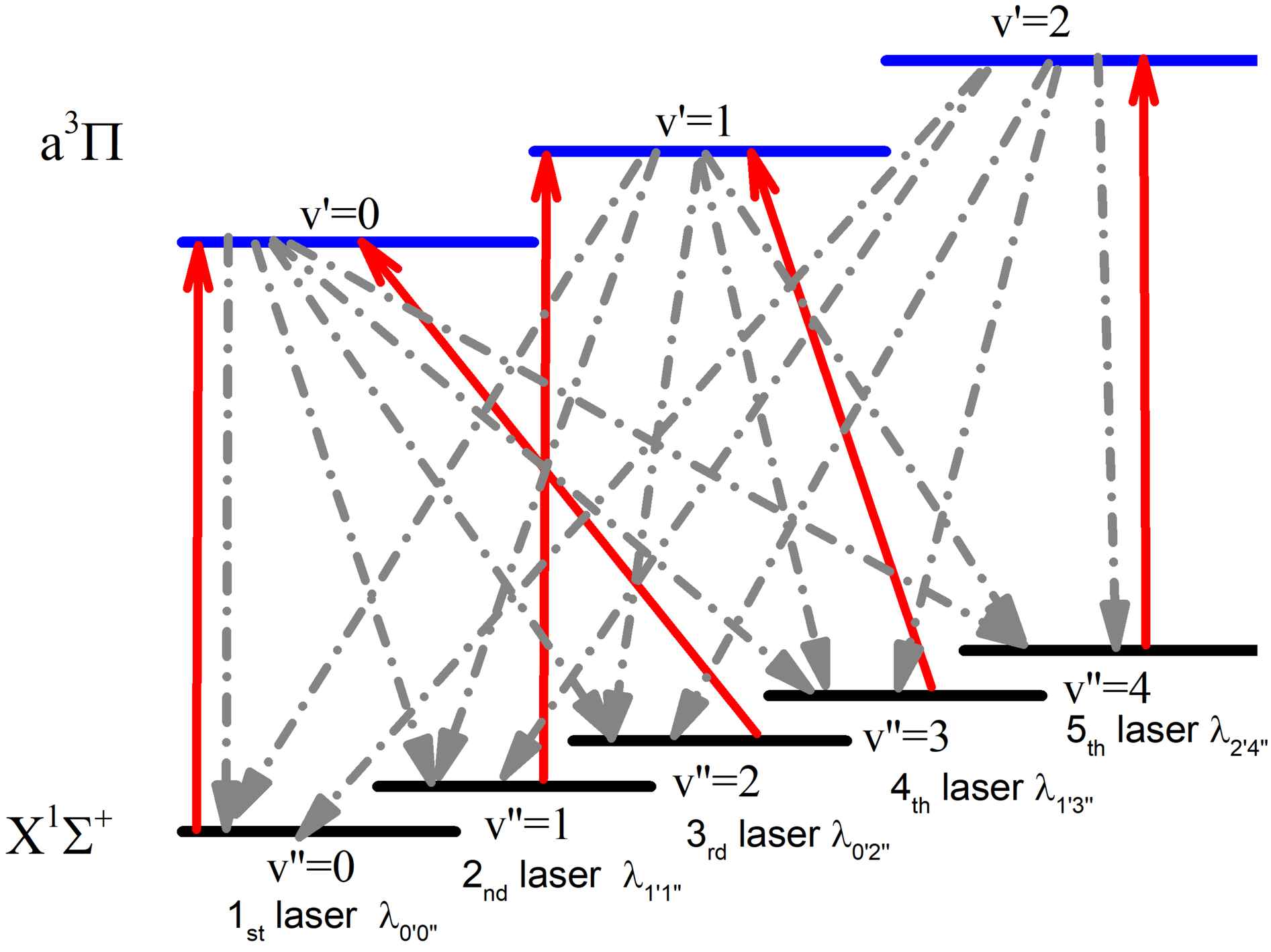

Accepted to J. Chem. Phys. 10.1063/5.0092620

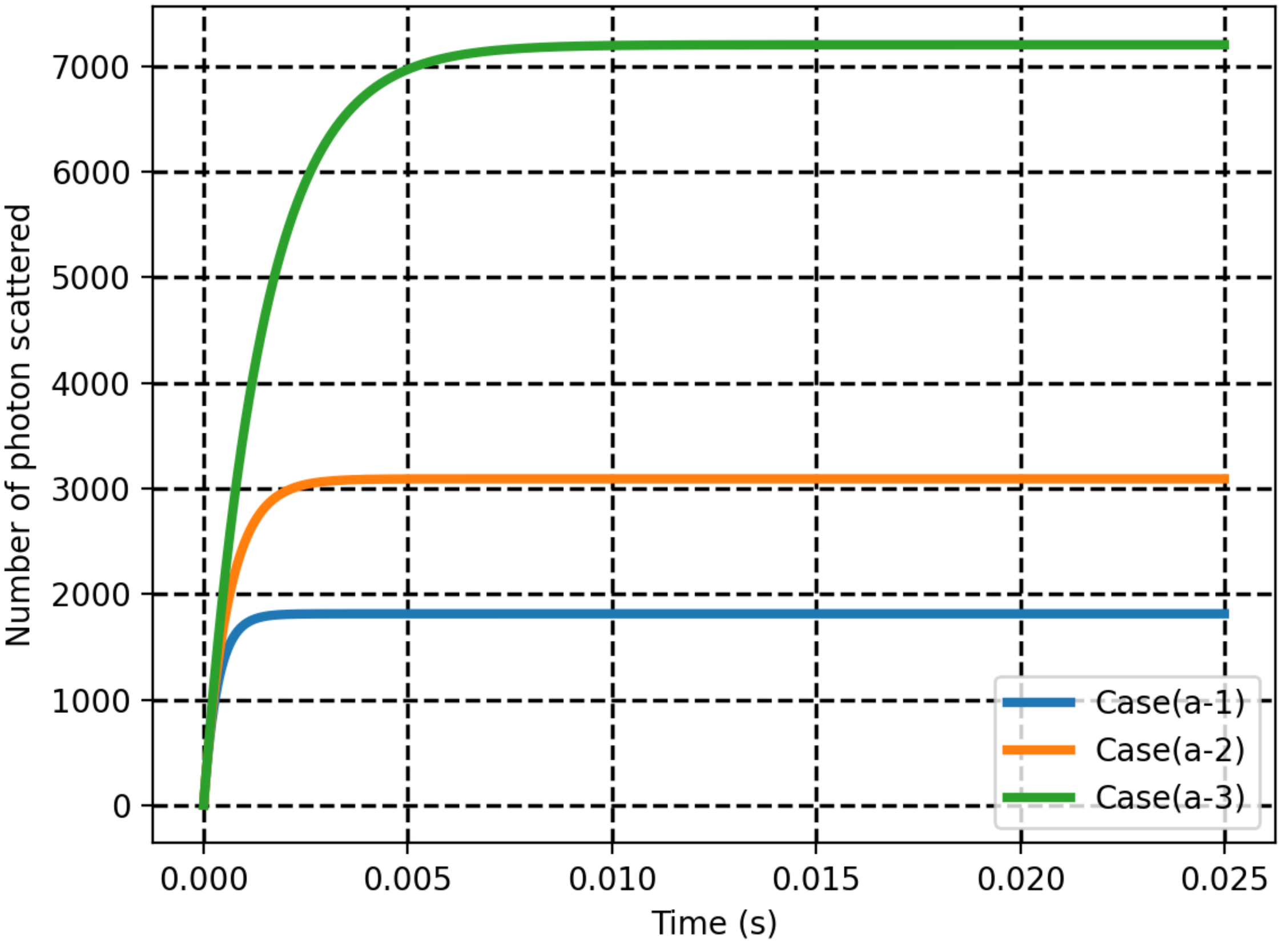

Accepted to J. Chem. Phys. 10.1063/5.0092620

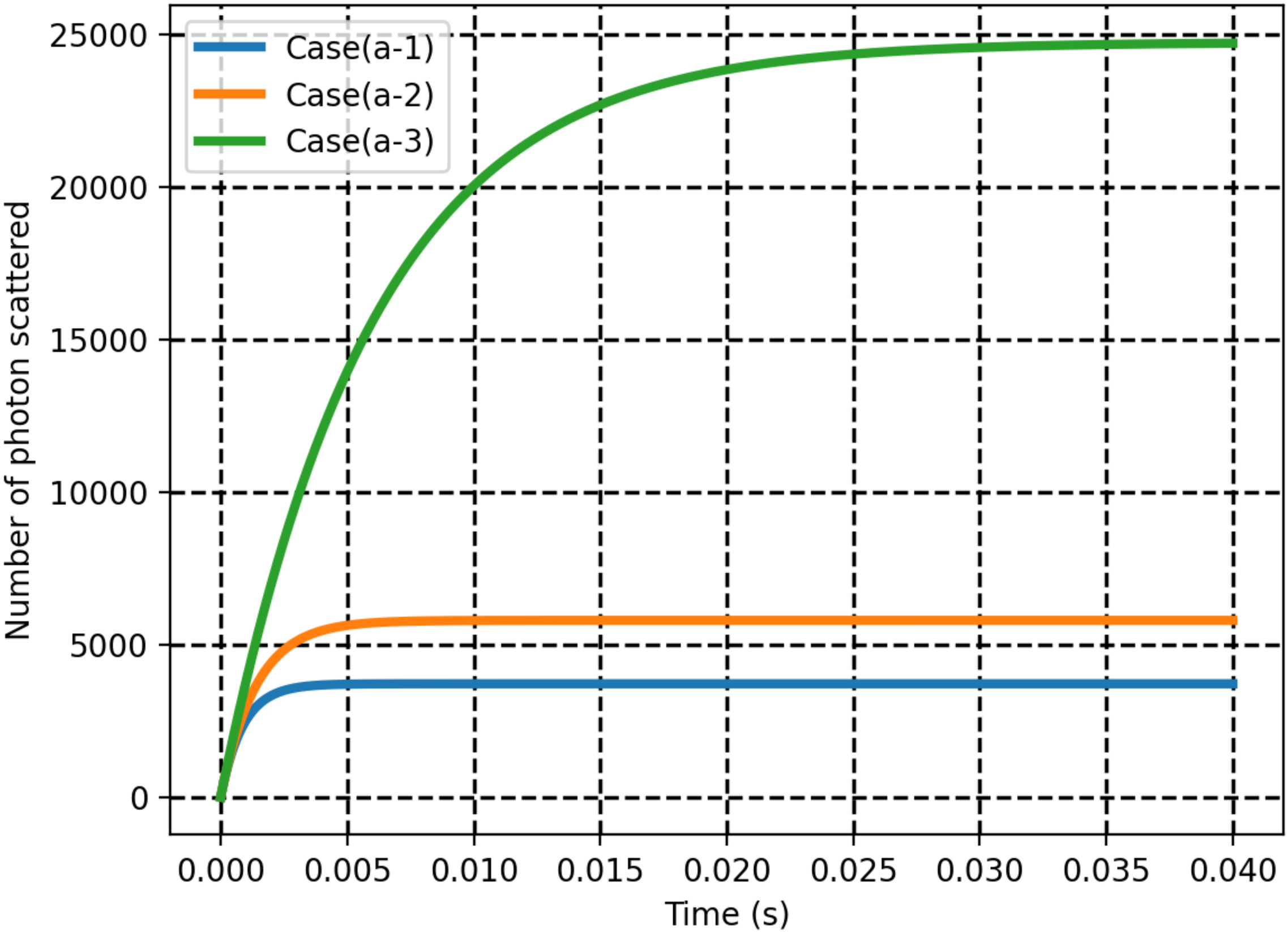

Accepted to J. Chem. Phys. 10.1063/5.0092620

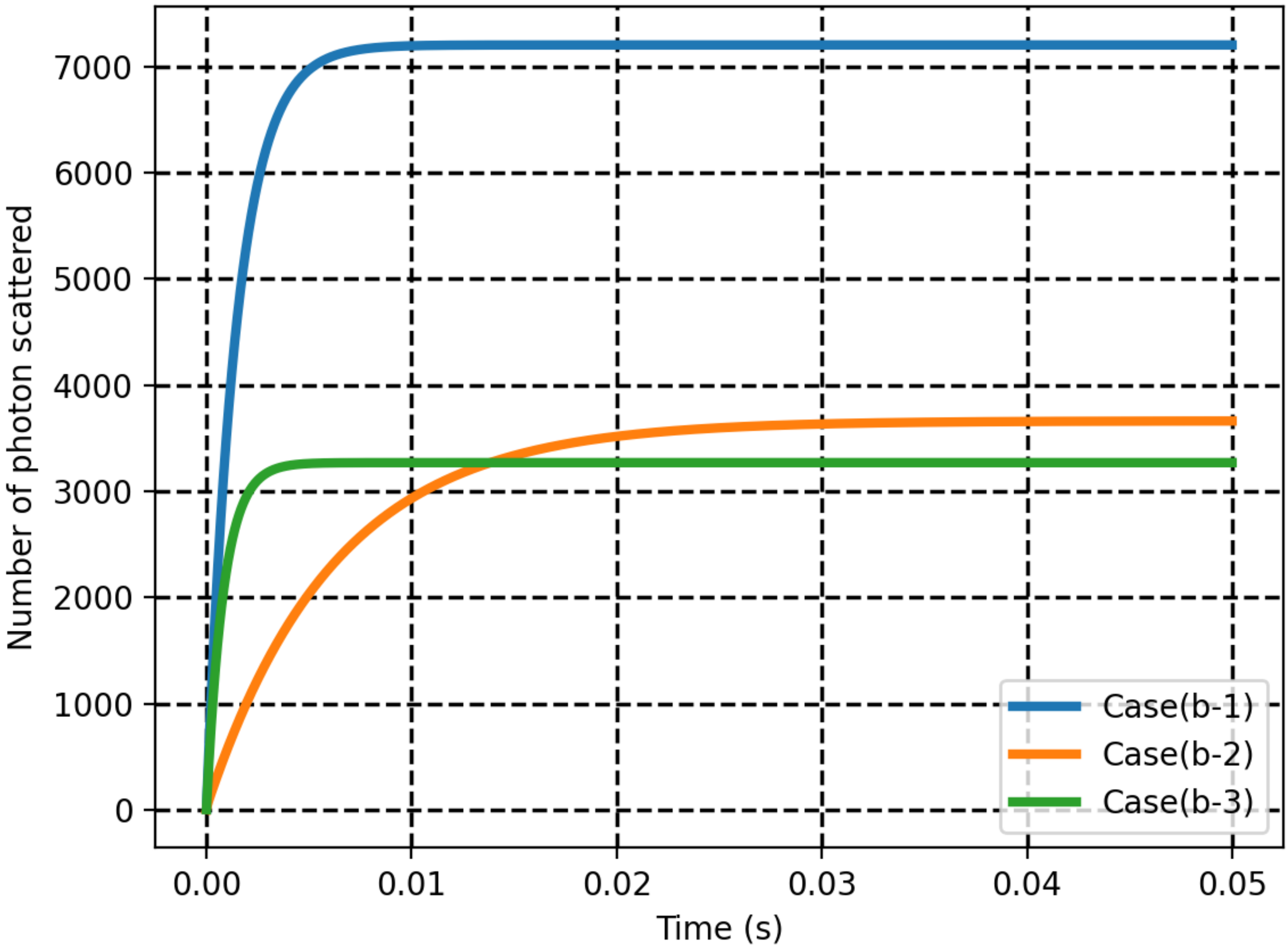

Accepted to J. Chem. Phys. 10.1063/5.0092620